Supporting Information

Antonyuk *et al.* 10.1073/pnas.0809170106

SI Text

Structure of ICSM 18 Fab. The structure of the Fab fragment of monoclonal antibody ICSM 18 was determined by molecular replacement to 1.57 Å resolution in space group $P2_12_12_1$ with 1 molecule (1 heavy and 1 light chain) in the asymmetric unit. The model refined to a final *R*-factor and *R*-free of 18.3% and 21.7%, respectively (Table 1), with an average mainchain atom B-factor of 18.3 Å^2, using TLS refinement (1). The final model contains 426 residues, of which 211 belong to the L chain and 215 to the H chain. The electron density maps allowed the modeling of all atoms in the structure, including several sidechains with double conformations, with *cis*-prolines modeled in positions 149, 151, and 191 of the H chain and 8, 94, and 120 of the L chain.

Structure of the PrP–ICSM 18 Fab Complex. The structure of the complex was solved by molecular replacement to 2.9 Å resolution in the $P6_322$ space group with 1 Fab and 1 PrP molecule in the asymmetric unit. The final *R*-factor was 21% and the *R*-free 26.9% (Table 1). The average B-factor for the model is 40 Å^2. The high quality of electron density (see Fig. S2) facilitated the tracing of a reliable model. The main changes of the Fab molecule on binding truncated PrP lie in the vicinity of the heavy-chain PrP-binding site (Fig. S4).

1. Winn MD, Isupov MN, Murshudov GN (2001) Use of TLS parameters to model anisotropic displacements in macromolecular refinement. *Acta Crystallogr D* 57:122–133.
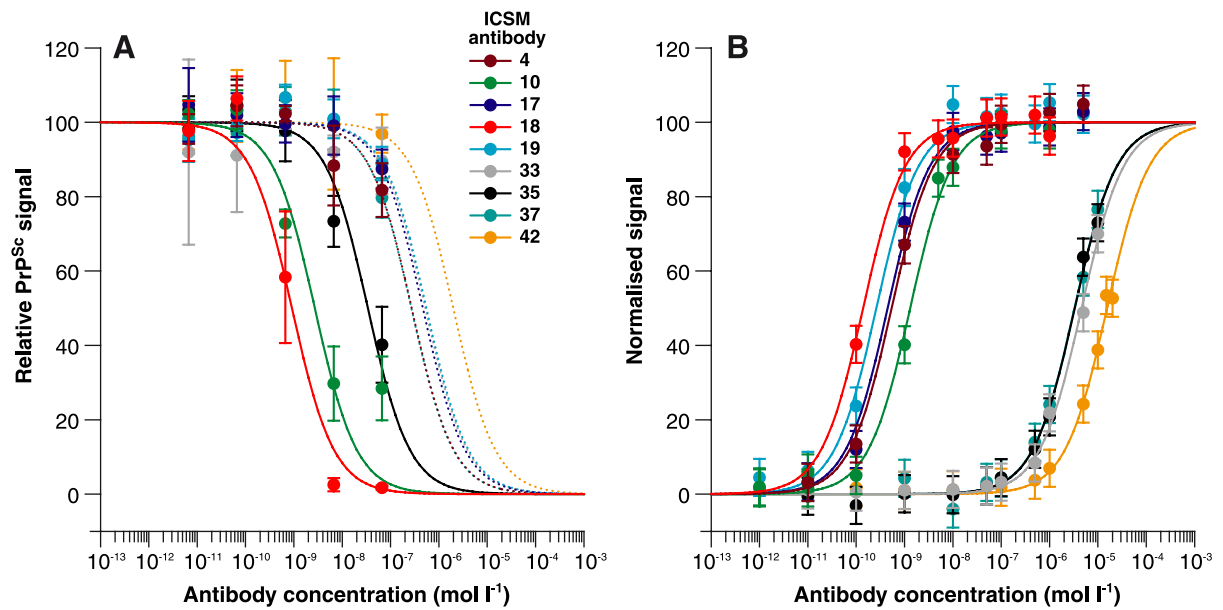
Fig. S1. Data for ICSM-antibody treatment of cells (*A*) and binding to recombinant PrP (*B*), as summarized in Fig. 1. (*A*) Fitted dose–response curves for the inhibition of PrP^{Sc} accumulation in ScN2a cells treated with various ICSM antibodies at the indicated concentrations. IC$_{50}$ values are listed in Table S1. Dashed lines indicate fitted curves that are ill-defined by the data. (*B*) Binding curves for the interactions between recombinant α-PrP and various ICSM antibodies determined by ELISA as described in *Methods*. K_d values are listed in Table S1.
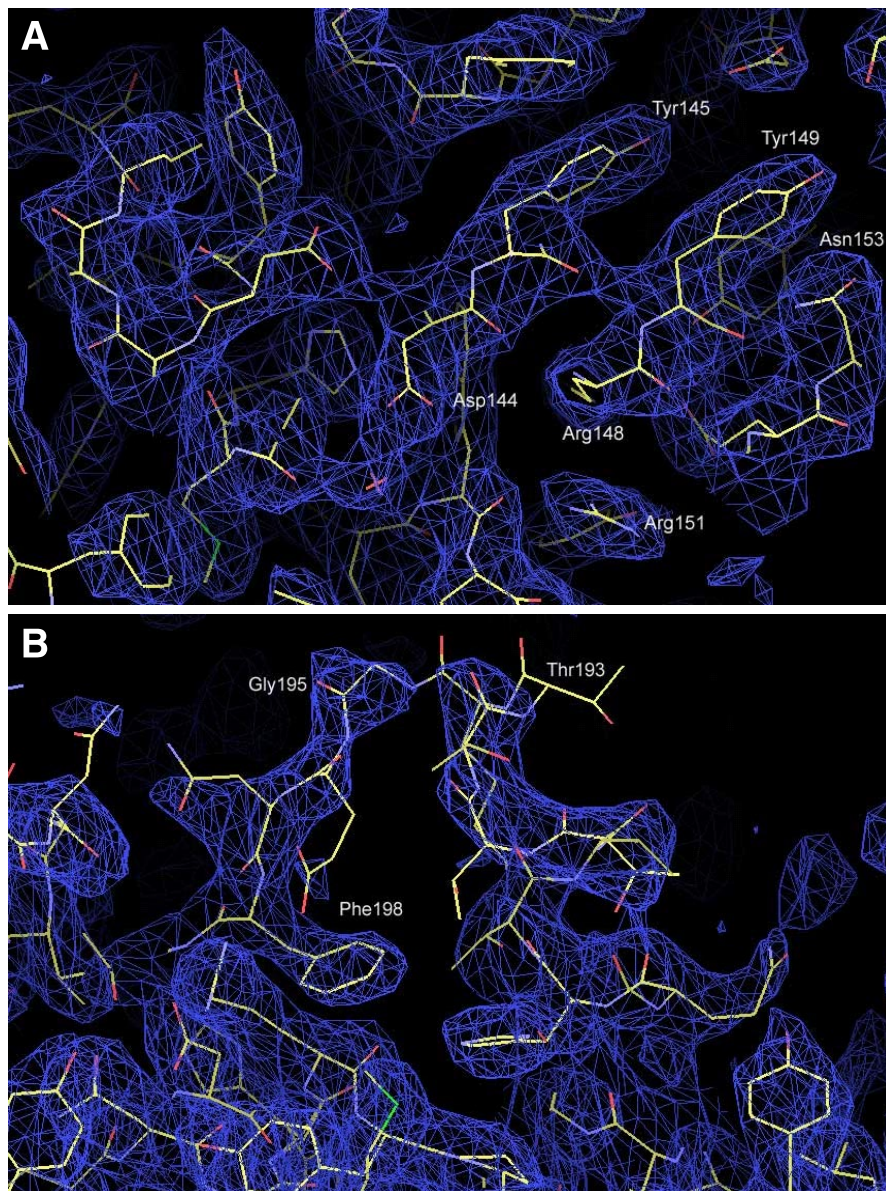
Fig. S2. The quality of the electron density maps for PrP in the complex at 2.9 Å-resolution. (*A*) The region of helix H1. (*B*) The most disordered part of the H2–H3 loop.
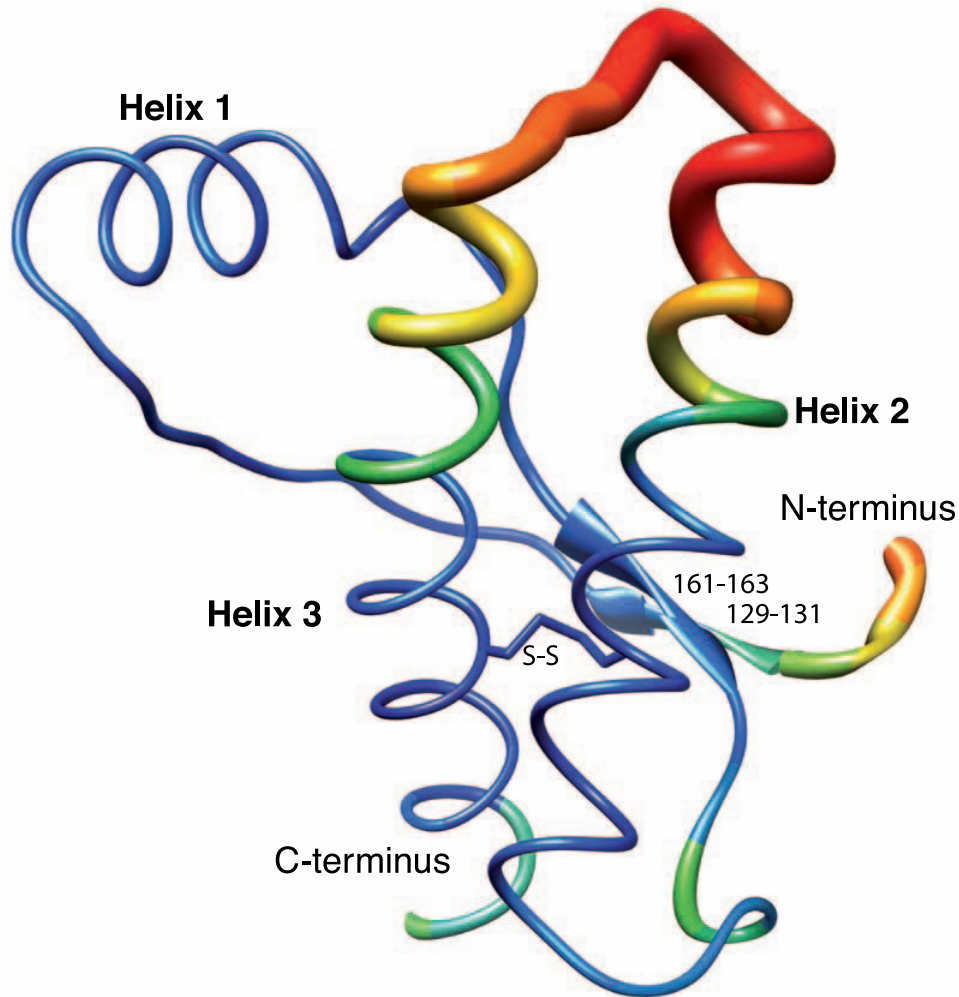
Fig. S3.   Thermal parameter distribution in human PrP$^{119-231}$ shown as B-factor ''putty'' as implemented in PyMol (www.pymol.org). The Cα atom B-factors range from 31 Å^2 to 58 Å^2 with average value 40 Å^2 and are depicted on the structure in dark blue (lowest B-factor) through to red (highest B-factor), with radius of the ribbon increasing from low to high B-factor. The lowest B-value is observed in the region of H2 and H3 where the disulfide bridge links the 2 helices (dark blue), with the next-most-stable region being H1 and the sequence between H1 and the 2 short β-strands. The largest B-factor is observed in the loop region linking helices H2 and H3 (red), where the electron density clearly shows more disorder than elsewhere in the structure.
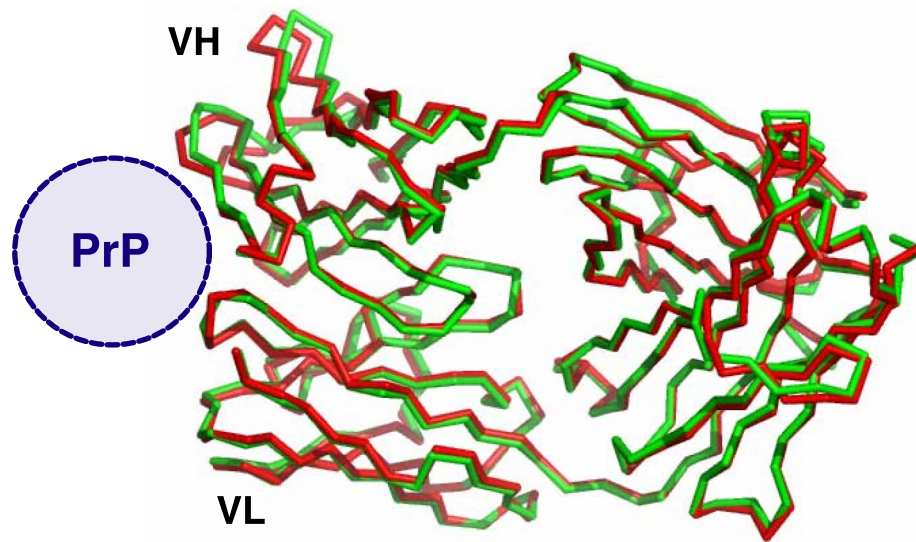
Fig. S4. The ICSM 18-Fab structure showing changes between free (red) and PrP-bound (green). The main change is in the H chain of the variable domain, VH. The rmsd between the Cα atoms in the 2 structures is 0.49 Å for 350 residues (0.8 Å overall).
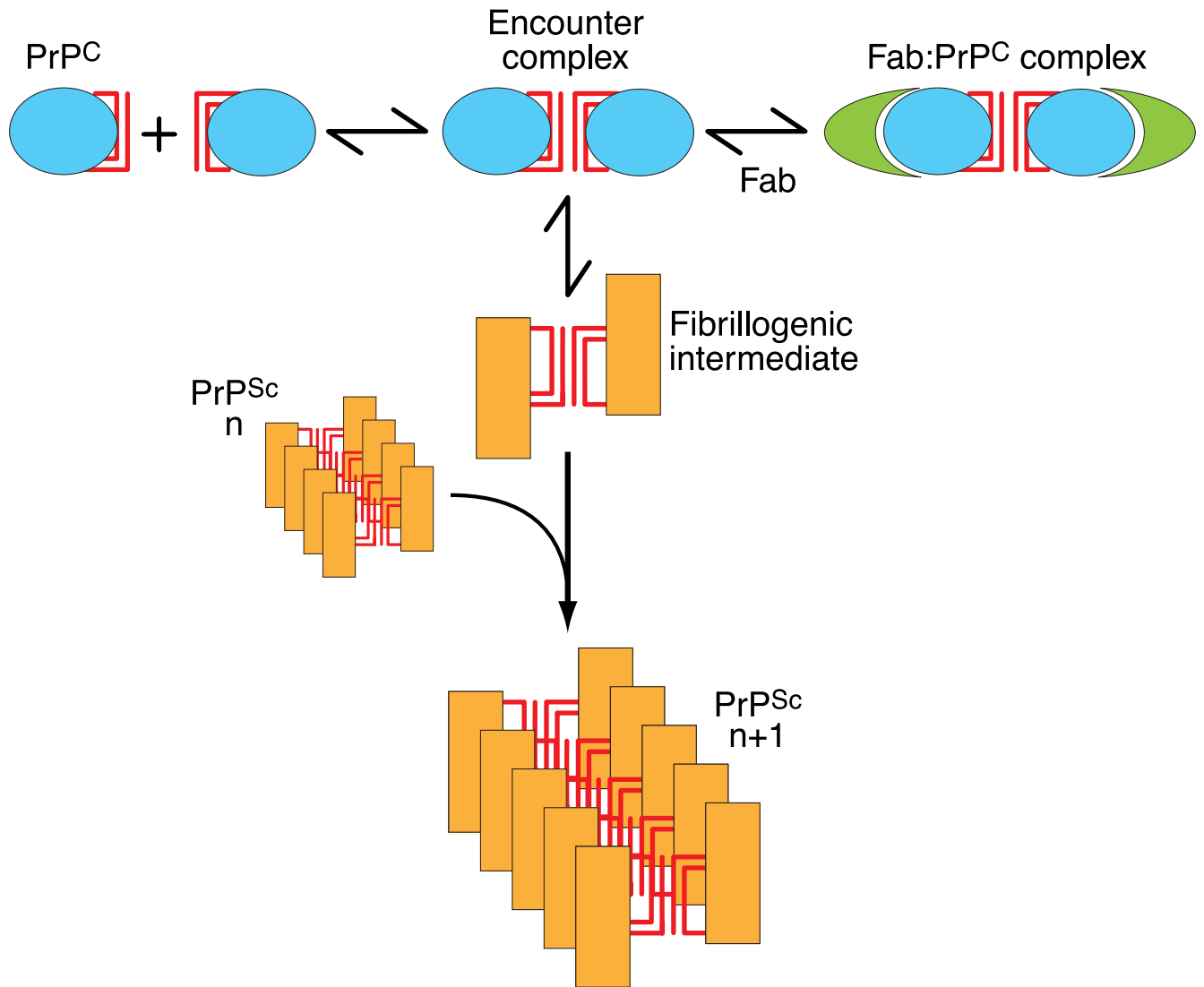
Fig. S5. Possible explanation for distinct PrP dimerization and inhibitory antibody contact domains. Two PrP^C molecules (α-helical region shown in blue) form an encounter complex by interactions between the β-strand structures (red). This (perhaps rare) encounter complex can undergo a rearrangement to a fibrillogenic state (orange) that can then add to a PrP^{Sc} particle with n dimers to form the $n + 1$ structure. Without interfering with the initial dimerization interface, the ICSM18 Fabs (green) could interact tightly with the PrP^C conformation (blue) and thereby prevent its conversion to the fibrillogenic form.

Table S1. Summary of IC$_{50}$s and K_ds for each antibody

Antibody	Immunogen	IC$_{50}$, M	K_d, M
ICSM 18	α-PrP	$7.5 \pm 1.9 \times 10^{-10}$	$1.3 \pm 0.1 \times 10^{-10}$
ICSM 10	α-PrP	$2.7 \pm 1.2 \times 10^{-9}$	$1.3 \pm 0.1 \times 10^{-9}$
ICSM 35	β-PrP	$4.0 \pm 1.1 \times 10^{-8}$	$3.3 \pm 0.2 \times 10^{-6}$
ICSM 37	β-PrP	$2.0 \pm 0.5 \times 10^{-7}$	$3.3 \pm 0.2 \times 10^{-6}$
ICSM 4	α-PrP	$3.0 \pm 1.5 \times 10^{-7}$	$5.4 \pm 0.7 \times 10^{-10}$
ICSM 19	α-PrP	$3.7 \pm 0.9 \times 10^{-7}$	$2.6 \pm 0.4 \times 10^{-10}$
ICSM 17	α-PrP	$4.7 \pm 1.3 \times 10^{-7}$	$4.2 \pm 0.6 \times 10^{-10}$
ICSM 33	β-PrP	$4.7 \pm 6.1 \times 10^{-7}$	$4.6 \pm 0.3 \times 10^{-6}$
ICSM 42	β-PrP	$1.4 \pm 2.0 \times 10^{-6}$	$1.5 \pm 0.1 \times 10^{-5}$

Summary of IC$_{50}$ and K_d values for each of the ICSM antibodies, as shown in Fig. S1, ranked according to IC$_{50}$. Values are mean $\pm$ SD of 2 or 3 independent experiments, determined as described.